Received 8 April 2024; revised 27 May 2024; accepted 23 June 2024. Date of publication 1 July 2024; date of current version 25 July 2024.

Digital Object Identifier 10.1109/OJCOMS.2024.3421518

Design of Low-Complexity Coded Modulation Employing High-Order QAM With Systematic Geometric Constellation Shaping

EITO KURIHARA [1] (Student Member, IEEE), AND HIDEKI OCHIAI [2] (Fellow, IEEE)

[1]Department of Electrical and Computer Engineering, Yokohama National University, Yokohama 240-8501, Kanagawa, Japan

[2]Graduate School of Engineering, Osaka University, Suita 565-0871, Osaka, Japan

CORRESPONDING AUTHOR: E. KURIHARA (e-mail: kurihara-eito-ms@ynu.jp)

This work was supported by the Japan Society for the Promotion of Science (JSPS) through the Grants-in-Aid for Scientific Research (KAKENHI) under Grant 21H04873.

ABSTRACT In this work, we investigate the performance of geometric constellation shaping for high-order coded quadrature amplitude modulation (QAM) over an additive white Gaussian noise (AWGN) channel. We focus on a systematic design where a single parameter uniquely determines the entire constellation points according to the truncated Gaussian distribution, and the parameter is optimized based on the resulting mutual information. Our main objective is to combine the proposed systematic geometric shaping with practical coded modulation so as to achieve high bandwidth efficiency with low design/decoding complexity. To this end, we investigate the use of multilevel coding (MLC) under multistage decoding (MSD) as well as bit-interleaved coded modulation (BICM), along with pulse amplitude modulation (PAM) consisting of as much as 128 signal points, i.e., leading to 16 384-ary QAM in the two-dimensional case. Our comparative studies employing the off-the-shelf binary punctured turbo codes show that, as we target higher spectral efficiency, MLC with MSD is more attractive than BICM in view of both bit error rate (BER) performance and decoding complexity. In addition, we introduce new closed-form bounds related to constellation constrained capacity, based on which one can quickly assess the capacity behavior of given discrete PAM constellations.

INDEX TERMS Bit-interleaved coded modulation (BICM), constellation constrained capacity bounds, geometric constellation shaping, multilevel coding (MLC), multistage decoding (MSD).

I. INTRODUCTION

DUE TO ever-increasing demands for high data-rate communications with limited spectral resources, bandwidth-efficient coded modulation schemes, especially in combination with higher-order modulations [1], would play an important role in future communications systems. Furthermore, in order to approach Shannon limit with a finite number of constellation points, the use of constellation shaping is essential [2].

Constellation shaping techniques have been investigated extensively so as to enhance achievable information rate at a given signal-to-noise power ratio (SNR). They can be classified into probabilistic shaping (e.g., [3], [4], [5]) and geometric shaping (e.g., [6], [7]), where the former attempts to control the probability distribution of the regular quadrature amplitude modulation (QAM) constellations, whereas the latter attempts to modify only the location of constellation points without controlling their distribution. Despite its significant potential gain, probabilistic shaping requires a *distribution matcher*, which typically increases the computational complexity of the transmitter [8]. To mitigate this issue, low-complexity implementations with short block codes have been studied in [9], [10]. Also, a combination of probabilistic and geometric shaping designed through machine learning has recently been considered in [11], [12]. This work focuses on geometric shaping since its complexity required for shaping operation is generally lower than that of probabilistic shaping, and it also has

high compatibility with the standard coded modulation schemes.

As for coded modulation, bit-interleaved coded modulation (BICM) [13], [14] and multilevel coding (MLC) with multistage decoding (MSD) [15] are the two representative approaches. BICM is a well-known approach that enjoys design simplicity with robustness against fading channels [14], [16]. Its major advantage from a viewpoint of practical implementation is that one can employ off-the-shelf capacity-approaching binary channel codes, such as turbo codes and low-density parity-check (LDPC) codes, without major modification of encoder and decoder. The main drawback of BICM is that its achievable information rate, which is characterized by bit-wise mutual information (BMI), is generally lower than the constellation constrained capacity. MLC is an alternative approach that can be operated with binary channel codes, where it can achieve channel capacity with MSD provided that the code rates of component codes are properly designed according to the information rates determined by the constellation constrained capacity [17]. Another major advantage of MLC/MSD in practice is that it can be employed with various binary channel codes that are available today. This is in contrast to trellis-coded modulation (TCM) [18], where the codes are designed over the Euclidean space and thus essentially non-binary. Nevertheless, designing MLC/MSD system with higher-order modulation is not straightforward due to a growing number of decoding stages. Therefore, the comparison between the two coded modulation schemes in view of achievable error rate performance as well as decoding complexity should be of great practical interest. We thus attempt to numerically compare these coded modulation schemes with geometric shaping.

The application of geometric shaping to MLC/MSD system has been investigated in [19], where hard decision decoding is employed in the higher levels so as to reduce overall decoding complexity [17], [20]. With application to BICM, a pseudo-Gaussian constellation design has been studied in [21], whereas the optimization of bit labeling is discussed in [22]. There have been several studies on constellation optimization with geometric shaping. Joint optimization of constellation and binary labeling based on simulated annealing (SA) has been proposed in [23], [24], whereas the applications of particle swarm optimization (PSO) algorithm and genetic algorithm (GA) have been investigated in [25] and [26], respectively. Also, an end-to-end learning of geometric shaping and probabilistic shaping has received significant recent attention in the field of optical fiber communications [27], [28].

In this work, we focus on a systematic approach where the constellation points can be uniquely determined by only a single parameter. More specifically, we modify Gaussian signaling similar to [21], [29], where the Gaussian distribution is first truncated to a specific level and then all the points are uniquely identified under certain statistical constraints. Thanks to this systematic design approach, the resulting constellation can be fully described with the single parameter. Therefore, unlike other numerical approaches that involve complex constellation optimization processes, our constellation can readily be reproduced and evaluated. We here attempt to optimize the parameter based on the constellation constrained capacity and the total BMI, which serve as achievable information rates for MLC/MSD and BICM, respectively.

The main drawback of our constellation design is that since it is based on a single dimension, its achievable shaping gain should be less than those optimized over multi-dimensional cases such as [30], [31], [32]. Nevertheless, these constellations require special and rather complicated set partitioning for MLC/MSD. For example, see [33] and [34] in the cases of two-dimensional non-square constellations such as hexagonal shell modulation (HSM) and amplitude-phase shift keying (APSK), respectively. It is thus challenging for high-dimensional constellations to achieve the constellation constrained capacity using binary channel coding in practice. On the other hand, if the constellation is a variant of the standard PAM having 2^m constellation points for a given positive integer m, then the application of MLC/MSD (with m levels) is rather straightforward. Such an approach has also been adopted in [35] in the framework of superposition coding.

In general, calculation of constellation constrained capacities requires numerical integration, which is often implemented by simulations such as Monte-Carlo integration. To circumvent this, their closed-form alternatives have been studied in the literature [36], [37], [38], and we also develop closed-form bounds that account for the loss of mutual information from its upper limit. Since these bounds are calculated without any numerical integration, they can be used for quickly assessing the capacity behavior as well as verifying the precise results obtained through numerical integration.

The main contributions of this work are summarized as follows:

- A systematic geometric constellation based on the truncated Gaussian distribution with a single parameter optimization is developed for high-order QAM constellations. The parameter is optimized based on the maximization of mutual information of the resulting constellation. We also compare our proposed constellations with those of [35] in terms of constellation constrained capacity, demonstrating the superiority of the proposed design in the case of one-dimensional constellation that can employ MLC/MSD with low-computational complexity.
- We compare the performance of BICM and MLC/MSD with the proposed geometric constellation shaping by extensive computer simulations employing the off-the-shelf binary punctured turbo codes in high spectral efficiency regime based on non-uniformly spaced QAM constellations with up to 16 384 constellation points. We

also meticulously evaluate the decoding complexity of both systems by quantifying the numbers of mathematical operations required for their bit-metric calculation. Our results show that MLC/MSD offers superior error rate performance and decoding complexity under the constraint that each code has the same codeword length.
- Two new closed-form expressions that serve as tight and loose bounds on the loss in constellation constrained capacity are developed. The accuracy of these bounds are examined by comparing with the precise value obtained by numerical integration.

The rest of this paper is organized as follows. In Section II, we first review the constellation constrained capacity and derive new bounds focusing on one-dimensional constellation, i.e., pulse-amplitude modulation (PAM). In Section III, we describe our systematic geometric shaping based on the truncated Gaussian distribution with optimization of a single parameter. The system models of MLC/MSD and BICM are briefly described in Section IV. The performance of these coded modulation systems with the proposed geometric shaping is compared through computer simulation in Section V, followed by the discussion of their decoding complexity in Section VI. Finally, Section VII concludes this work.

We note that some initial results on the constellation shaping based on the truncated Gaussian distribution in this paper were presented in [39].

II. CLOSED-FORM BOUNDS FOR LOSS IN CONSTELLATION CONSTRAINED CAPACITY

We first review a mathematical expression of constellation constrained capacity for arbitrary discrete constellations. Throughout this work, we focus on a practical framework where the two orthogonal channels, i.e., in-phase (I) and quadrature (Q) channels, are designed independently as in the case of the standard QAM. Therefore, we analyze the constellation constrained capacity of PAM as its application to the two-dimensional case is straightforward (i.e., it is twice as much as the one-dimensional capacity with appropriate scaling of SNR).

To date, derivation of simple approximate expressions or bounds for constellation constrained capacity remains one of the continuing challenges in signal constellation design. An approximate expression for the mutual information of extremely dense PAM (referred to as ∞-*PAM*) has been considered in [36], whereas a closed-form upper bound for the constellation constrained capacity of QAM has been derived through the sphere-packing argument in [37]. Also, capacity of pulse-position modulation (PPM) is discussed in [38], where its simple upper bound based on Jensen's inequality has been proposed as a performance measure of ultra-wideband communications. In this section, we derive closed-form bounds focusing on the loss from the capacity limit of PAM.

A. CONSTELLATION CONSTRAINED CAPACITY

We consider the following real-valued discrete-time AWGN channel:

$$Y = X + Z, \tag{1}$$

where Y is the received symbol and Z is the AWGN term with zero mean and variance $\sigma^2 = N_0/2$, i.e., $Z \sim \mathcal{N}(0, \sigma^2)$. The transmitted symbol X is chosen from the PAM constellation set $\mathcal{A} = \{a_0, a_1, \ldots, a_{M-1}\}$, where $M = 2^m$ is the number of constellation points in one dimension and the positive integer m corresponds to the number of uncoded bits transmitted by each PAM symbol. We denote the average energy of the transmitted PAM symbol by $E_s/2$, with E_s representing that of QAM. We also assume that all the constellation points are equally probable, i.e., $P_X(a_k) \triangleq P(X = a_k) = 1/M$ for $\forall k = \{0, 1, \ldots, M-1\}$. The conditional probability distribution function (PDF) of the received symbol Y given that the symbol $X = a$ is transmitted is written by

$$p_{Y|X}(y \mid a) = \frac{1}{\sqrt{2\pi\sigma^2}} e^{-\frac{(y-a)^2}{2\sigma^2}}. \tag{2}$$

Under the above model, the mutual information between the transmitted symbol and the received symbol over an AWGN channel, often called *coded modulation capacity*, is expressed in terms of the constellation set $\mathcal{A}$ and the channel SNR, E_s/N_0, as [18]

$$C_{\mathrm{CM}}\left(\mathcal{A}, \frac{E_s}{N_0}\right) = \mathbb{E}_{Y,X}\left[\log_2 \frac{p_{Y|X}(Y \mid X)}{p_Y(Y)}\right] \tag{3}$$

in bits per dimension, where $\mathbb{E}[\,\cdot\,]$ denotes an expectation operation with its subscript(s) representing the random variable(s) over which the expectation is performed. The above equation can also be expressed, omitting the dependence on $\mathcal{A}$ and E_s/N_0 for simplicity, as

$$C_{\mathrm{CM}} = m - \frac{1}{M}\sum_{k=0}^{M-1} \mathbb{E}_Z\left[\log_2\left\{\sum_{l=0}^{M-1} e^{-\frac{2Z(a_k-a_l)+(a_k-a_l)^2}{2\sigma^2}}\right\}\right]. \tag{4}$$

As a consequence, the constellation constrained capacity for PAM is expressed as

$$C_{\mathrm{CM}} = m - \underbrace{\mathbb{E}_Z[\psi(Z)]}_{\triangleq\, \xi}, \tag{5}$$

with

$$\psi(Z) \triangleq \frac{1}{M}\sum_{k=0}^{M-1} \log_2\left\{\sum_{l=0}^{M-1} e^{-\frac{a_k-a_l}{\sigma^2}Z - \frac{(a_k-a_l)^2}{2\sigma^2}}\right\}. \tag{6}$$

Note that the quantity ξ defined in (5) corresponds to the reduction of capacity from its upper limit of $m = \log_2 M$. While this upper limit is determined only by M, i.e., the number of constellation points, the term ξ depends on the constellation points $\mathcal{A}$. Therefore, it serves as an alternative measure equivalent to the constellation constrained capacity. In general, however, calculation of ξ requires expectation

with respect to Z, and this may not be expressed in closed form. As a result, numerical integration should be necessary, where its accuracy depends on the precision of numerical calculation. To circumvent this, we will develop two closed-form lower bounds for ξ, depending on the geometric property of PAM constellations. They may serve as alternative measures for assessing the reduction of information rate associated with given constellation points without resorting to numerical integration.

B. DERIVATION OF BOUNDS

We attempt to find two lower bounds to the measure ξ defined in (5). To this end, we first show that the function $\psi(Z)$ defined in (6) is convex for $Z \geq 0$. Note that $\psi(Z)$ can be rewritten as

$$\psi(Z) = \frac{1}{M}\sum_{k=0}^{M-1} \log_2\left(1 + \sum_{\substack{l=0\\ l\neq k}}^{M-1} \alpha_l e^{A_l Z}\right), \tag{7}$$

where

$$\alpha_l \triangleq e^{-\frac{(a_k-a_l)^2}{2\sigma^2}}, \quad A_l \triangleq \frac{a_l - a_k}{\sigma^2}. \tag{8}$$

Therefore, it is sufficient to show that the following function

$$g(x) = \ln\left(1 + \sum_l \alpha_l e^{A_l x}\right), \quad \text{for} \quad \alpha_l \geq 0, A_l \in \mathbb{R}, \tag{9}$$

is convex for $x \geq 0$. Since the second derivative of $g(x)$ is expressed as

$$g''(x) = \frac{\sum_l \alpha_l A_l^2 e^{A_l x} + \sum\sum_{i<l} \alpha_i \alpha_l (A_i - A_l)^2 e^{(A_i+A_l)^2}}{\left(1 + \sum_l \alpha_l e^{A_l x}\right)^2}, \tag{10}$$

it follows that $g''(x) \geq 0$ for $x \geq 0$, and thus $\psi(Z)$ is convex for $Z \geq 0$.

1) A LOOSE BOUND FOR GENERAL PAM

Since $\psi(Z)$ is convex for $Z \geq 0$, by Jensen's inequality we have

$$\xi = \mathbb{E}_Z[\psi(Z)] \geq \psi(\mathbb{E}_Z[Z]) = \psi(0) \triangleq \xi_L, \tag{11}$$

where ξ_L corresponds to the *loose* lower bound to ξ. It thus can be expressed as

$$\xi_L = \frac{1}{M}\sum_{k=0}^{M-1} \log_2\left\{1 + \sum_{\substack{l=0\\ l\neq k}}^{M-1} e^{\frac{(a_k-a_l)^2}{2\sigma^2}}\right\}, \tag{12}$$

which does not require any numerical integration for its calculation.

2) A TIGHTER BOUND FOR SYMMETRIC PAM

In practice, PAM constellations are designed to be origin-symmetric, i.e.,

$$a_k = -a_{(M-1)-k}, \quad \text{for} \quad \forall k \in \{0, 1, \ldots, M/2-1\}. \tag{13}$$

When the above relationship holds, then we can derive a tighter lower bound to ξ.

To this end, we first notice that with the condition (13), $\psi(Z)$ is expressed as

$$\begin{aligned}
\psi(Z) &= \sum_{k=0}^{M/2-1}\left[\log_2\left\{\sum_{l=0}^{M-1} e^{-\frac{(a_k-a_l)}{\sigma^2}Z - \frac{(a_k-a_l)^2}{2\sigma^2}}\right\}\right.\\
&\qquad \left. + \log_2\left\{\sum_{l=0}^{M-1} e^{-\frac{(a_{M-1-k}-a_l)}{\sigma^2}Z - \frac{(a_{M-1-k}-a_l)^2}{2\sigma^2}}\right\}\right]\\
&= \sum_{k=0}^{M/2-1}\left[\log_2\left\{\sum_{l=0}^{M-1} e^{-\frac{(a_k-a_l)}{\sigma^2}Z - \frac{(a_k-a_l)^2}{2\sigma^2}}\right\}\right.\\
&\qquad \left. + \log_2\left\{\sum_{l=0}^{M-1} e^{-\frac{(a_k-a_l)}{\sigma^2}(-Z) - \frac{(a_k-a_l)^2}{2\sigma^2}}\right\}\right]\\
&= \psi(-Z),
\end{aligned} \tag{14}$$

which means that $\psi(Z)$ is an even function. We may thus write

$$\xi = \mathbb{E}_Z[\psi(Z)] = \mathbb{E}_Z[\psi(|Z|)] \geq \psi(\mathbb{E}_Z[|Z|]) \triangleq \xi_T, \tag{15}$$

where ξ_T corresponds to the *tighter* lower bound to ξ. Noticing that

$$\begin{aligned}
\mathbb{E}_Z[|Z|] &= \int_{-\infty}^{\infty} \frac{|z|}{\sqrt{2\pi\sigma^2}} e^{-\frac{z^2}{2\sigma^2}} dz\\
&= 2\int_0^{\infty} \frac{z}{\sqrt{2\pi\sigma^2}} e^{-\frac{z^2}{2\sigma^2}} dz = \sqrt{\frac{2\sigma^2}{\pi}},
\end{aligned} \tag{16}$$

we may express ξ_T in closed form as

$$\xi_T = \frac{1}{M}\sum_{k=0}^{M-1} \log_2\left\{1 + \sum_{\substack{l=0\\ l\neq k}}^{M-1} e^{-(a_k-a_l)\sqrt{\frac{2}{\pi\sigma^2}} - \frac{(a_k-a_l)^2}{2\sigma^2}}\right\}, \tag{17}$$

which can easily be calculated without numerical integration.

C. NUMERICAL COMPARISON

Fig. 1 compares the numerical values of ξ with the corresponding two lower bounds ξ_L, ξ_T in the case of the standard (uniformly-spaced) PAM constellations with $M = 16, 32, 64$, and 128. It can be observed that the derived bound ξ_T (dot-dashed lines) is tighter than ξ_L (dotted lines) as expected. Note that from (5), we may express an upper bound of the constellation constrained capacity as $C_{\mathrm{CM}} \leq m - \xi_T \leq m - \xi_L$ for $m = \log_2 M$. Unfortunately, these bounds may not be necessarily informative as they may exceed the theoretical limit (i.e., Shannon limit) in low SNR regions of interest. Nevertheless, the bounds ξ_T and ξ_L themselves may serve as useful indicators in terms of degradation from the upper

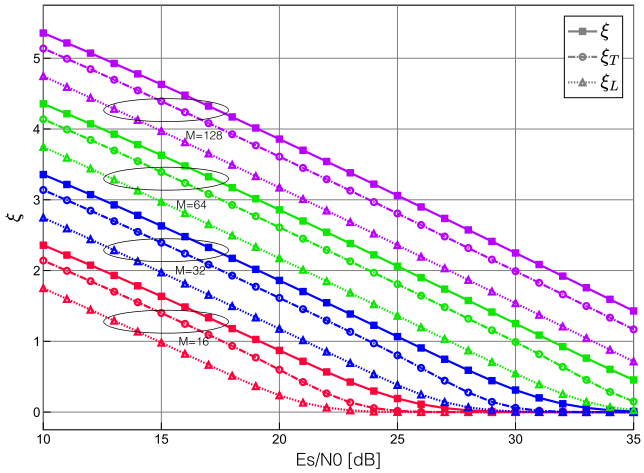

FIGURE 1. Comparison of the measure ξ calculated through numerical integration and the two closed-form lower bounds ξ_L, ξ_T in the case of the standard PAM constellations.

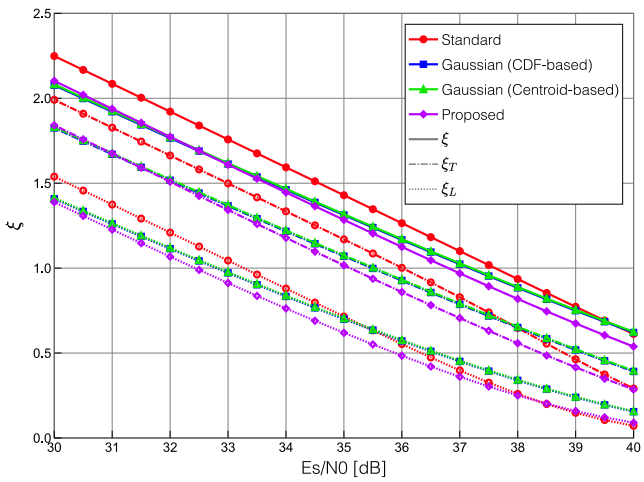

FIGURE 2. Comparison of the measure ξ and the two closed-form lower bounds ξ_L, ξ_T applied to the four different 128-PAM constellations.

limit of capacity for a given set of discrete constellation points, as opposed to the Shannon limit which results from (continuous) Gaussian distribution.

Fig. 2 compares the numerical values of ξ and the corresponding closed-form bounds ξ_T and ξ_L for each of the four different 128-PAM constellations according to their specific design approaches described in the next section. It is observed from these results that one can largely assess the performance gaps among different discrete constellations by the proposed closed-form numerical measures ξ_T and ξ_L.

III. SYSTEMATIC GEOMETRIC CONSTELLATION SHAPING

While it is well known that the optimal constellation over an AWGN channel under the average signal power constraint is Gaussian, the number of constellation points should be finite in practical systems, and uniformly-spaced PAMs (QAMs) are often adopted. To improve their achievable information rate without any major additional complexity, geometric shaping approaches focusing on Gaussian-like discrete constellations have been proposed in the literature. In particular, the centroid-based approach is suggested in [40] and cumulative distribution function (CDF)-based approach is considered in [41]. In this section, we describe these constellation designs and analyze their performance in terms of capacity and peak-to-average power ratio (PAPR). We also introduce a systematic constellation design approach based on the truncated Gaussian distribution, where a single parameter balances the two extreme constellations represented by the standard (uniform) and Gaussian distributions.

A. CONVENTIONAL CONSTELLATION DESIGN

1) STANDARD PAM

We first describe the standard M-ary PAM constellations where the adjacent points have equal Euclidean distance. Let $\mathcal{A} = \{a_0, a_1, \ldots, a_{M-1}\}$ denote the constellation points of general PAM. In the case of the standard PAM, we have

$$a_k = (-M + 1 + 2k)d, \quad k \in \{0, 1, \ldots, M-1\}, \quad (18)$$

with

$$d = \sqrt{\frac{3}{2(M^2-1)}}. \quad (19)$$

Note that $2d$ corresponds to the minimum Euclidean distance of the constellation points, and since we assume that the probability distribution of each constellation point is equal, i.e., $P_X(a_k) = 1/M$ for $\forall k \in \{0, 1, \ldots, M-1\}$, the average energy is normalized such that $\mathbb{E}[X^2] = E_s/2$. Note also that without loss of generality, we set $E_s = 1$ in what follows.

2) GAUSSIAN-LIKE PAM (CENTROID-BASED APPROACH)

We review the approach based on the centroid [40], where we first divide the entire region $(-\infty, \infty)$ into M sub-regions such that the probability of selecting each sub-region is equal (i.e., $1/M$), and set the constellation point of each sub-region as its expected value (i.e., the *centroid*). More specifically, we divide the zero-mean Gaussian probability density function (PDF), $\mathcal{N}(0, \sigma^2)$, where σ^2 represents its variance, into M disjoint sub-regions, where the kth sub-region is given by $\mathcal{R}_k = (R_k, R_{k+1})$ with the boundary conditions $R_0 = -\infty$ and $R_M = \infty$. Since the signal should fall on one of the M sub-regions with equal probability, we have

$$\int_{R_k}^{R_{k+1}} \frac{1}{\sqrt{2\pi\sigma^2}} e^{-\frac{x^2}{2\sigma^2}} dx = \frac{1}{M}, \quad k \in \{0, 1, \ldots, M-1\}. \quad (20)$$

It follows that

$$R_k = \sqrt{2\sigma^2}\, \mathrm{erf}^{-1}\left(\frac{2k}{M} - 1\right), \quad (21)$$

where $\mathrm{erf}(\cdot)$ is the error function and thus $\mathrm{erf}^{-1}(\cdot)$ is its inverse function. With $X \sim \mathcal{N}(0, \sigma^2)$, the signal point in each sub-region can be uniquely determined by its conditional expectation as

$$\begin{aligned}\hat{a}_k &= \mathbb{E}[X \mid X \in \mathcal{R}_k], \\ &= \frac{M}{\sqrt{2\pi\sigma^2}}\left(e^{-\frac{R_k^2}{2\sigma^2}} - e^{-\frac{R_{k+1}^2}{2\sigma^2}}\right) \\ &= \frac{M}{\sqrt{2\pi\sigma^2}}\left(e^{-\left[\mathrm{erf}^{-1}\left(\frac{2k}{M}-1\right)\right]^2} - e^{-\left[\mathrm{erf}^{-1}\left(\frac{2(k+1)}{M}-1\right)\right]^2}\right). \quad (22)\end{aligned}$$

Since the set of the constellation points $\{\hat{a}_0, \hat{a}_1, \ldots, \hat{a}_{M-1}\}$ does not meet the energy constraint, we scale them as

$$a_k \triangleq \frac{\hat{a}_k}{\sqrt{\frac{2}{M}\sum_{k=0}^{M-1}\hat{a}_k^2}} \quad (23)$$

such that the resulting constellation $\{a_0, a_1, \ldots, a_{M-1}\}$ satisfies $\mathbb{E}[X^2] = 1/2$.

3) GAUSSIAN-LIKE PAM (CDF-BASED APPROACH)

In [41], a simple approach of generating Gaussian-like discrete constellation is developed. In this case, each tentative constellation point is chosen such that its CDF value is equally spaced. Specifically, let $X \sim \mathcal{N}(0, \frac{1}{2})$ with its CDF $F_X(x)$ given by

$$F_X(x) = P(X \le x) = \frac{1 + \mathrm{erf}(x)}{2}. \quad (24)$$

The kth tentative constellation point $\hat{a}_k$ should be chosen such that

$$F_X(\hat{a}_k) = \frac{k + \frac{1}{2}}{M}, \quad k \in \{0, 1, \ldots, M-1\}. \quad (25)$$

Thus, we obtain the kth tentative constellation point as

$$\hat{a}_k = \mathrm{erf}^{-1}\left(\frac{2k+1}{M} - 1\right). \quad (26)$$

We finally scale the magnitude of constellation according to (23) and obtain the desired points $\{a_0, a_1, \ldots, a_{M-1}\}$.

The above two Gaussian-like constellations with $M = 32$ are compared in Fig. 3 as M^2-QAM, where we observe a slight difference especially in their dynamic range. As we will see later, the CDF-based approach has an advantage in terms of achievable information rate (in addition to its lower PAPR) over the centroid-based approach, despite its simpler expression. Thus, in the next subsection, we will focus on the constellation design based on modification of the CDF-based approach.

B. PROPOSED CONSTELLATION DESIGN

We propose a constellation design according to the CDF-based approach where the reference CDF is modified according to the *truncated* Gaussian distribution. We first introduce a new coefficient b, which limits the effective range of the Gaussian PDF to $(-b, b)$. According to (24), the probability that the signal is below b can be expressed as

$$F_X(b) = \frac{1 + \mathrm{erf}(b)}{2}. \quad (27)$$

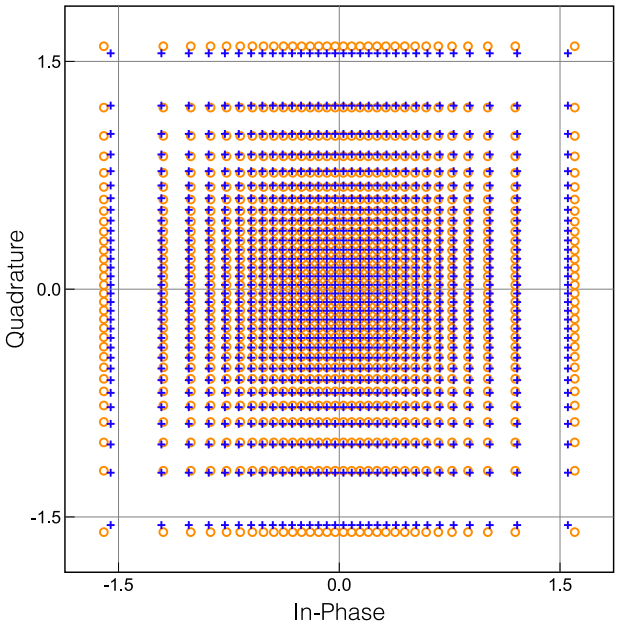

FIGURE 3. Comparison of two Gaussian-like constellations (1024-QAM); The orange circles and blue crosses represent those designed by the centroid-based and CDF-based approaches, respectively.

Then, the effective range of the CDF should be scaled from $[0, 1]$ to $[F_X(-b), F_X(b)]$, and thus the kth tentative constellation point should be chosen such that

$$\begin{aligned}F_X(\hat{a}_k) &= \frac{1 + \mathrm{erf}(\hat{a}_k)}{2} \\ &= (F_X(b) - F_X(-b))\frac{k + \frac{1}{2}}{M} + F_X(-b). \quad (28)\end{aligned}$$

After some manipulations, we obtain the kth tentative signal point as

$$\hat{a}_k = \mathrm{erf}^{-1}\left(\alpha\left(\frac{2k+1}{M} - 1\right)\right), \quad (29)$$

with

$$\alpha \triangleq \mathrm{erf}(b), \quad \alpha \in [0, 1], \quad (30)$$

which is used as our shaping parameter. Finally, the desired constellation points $\{a_0, a_1, \ldots, a_{M-1}\}$ are obtained according to the normalization, i.e., (23).

The transition of 32-PAM constellation points (i.e., 1024-QAM) designed by this approach along with the parameter α is plotted in Fig. 4, where we observe that the signal points closely resemble the Gaussian distribution as α increases up to 1. On the other hand, they approach the standard (i,e,. uniformly spaced) 32-PAM as α approaches 0 since, in that case, the PDF within the effective range $(-b, b)$ can be considered to be flat (constant) in the limit of $b \to 0$.

C. NUMERICAL ANALYSIS

1) CAPACITY ANALYSIS

We numerically evaluate the above designed 32-PAM constellations in terms of both the constellation constrained

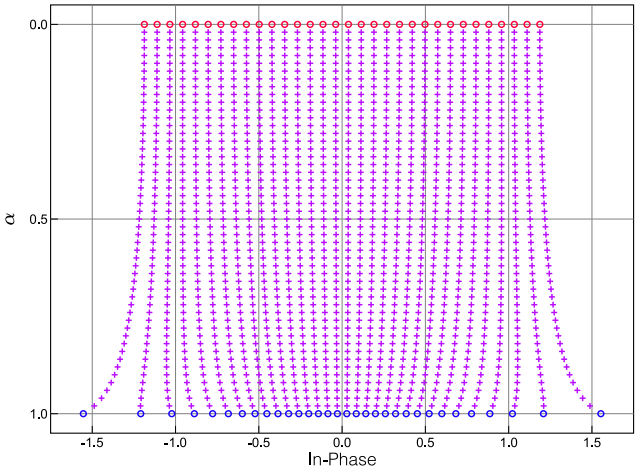

FIGURE 4. Transition of the shaped constellation points in the case of 32-PAM with respect to the design parameter α.

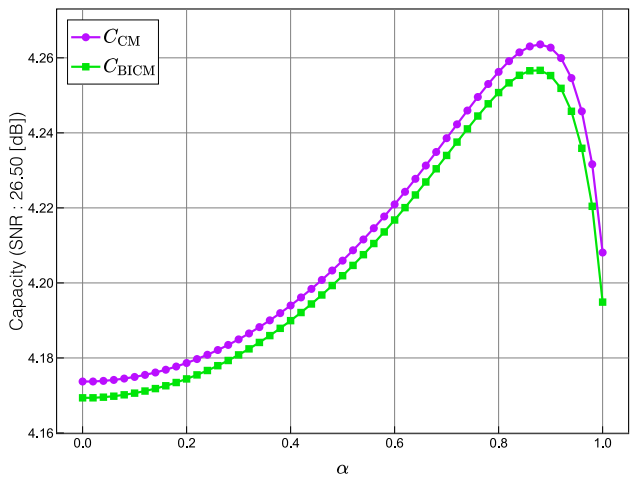

FIGURE 5. Comparison of CM and BICM capacity in case of the shaped 32-PAMs with respect to the design parameter α.

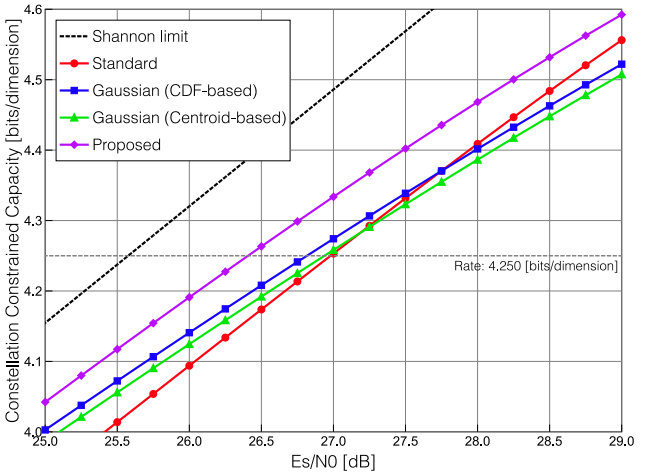

FIGURE 6. Comparison of the conventional and proposed 32-PAMs in terms of their constellation constrained capacity.

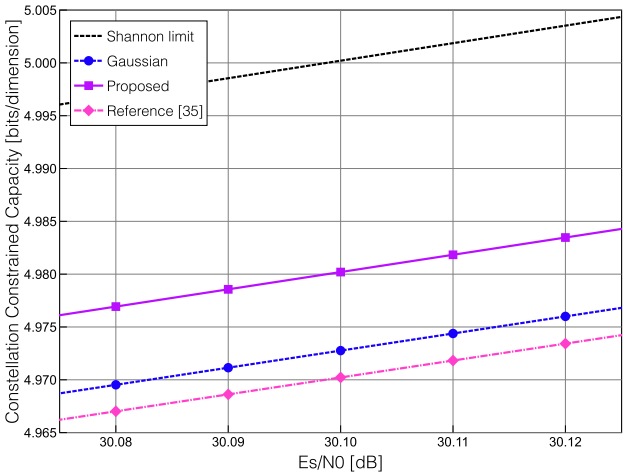

FIGURE 7. Comparison of the proposed 256-PAMs and that based on [35] in terms of their constellation constrained capacity.

capacity and total bit-wise mutual information (BMI), where the latter is often called BICM capacity (denoted by C_{BICM} in what follows), and considered as the ideal information rate achieved by BICM system at a given SNR. (The precise definition will be described later in Section IV-B.) The results are shown as a function of α in Fig. 5, where the SNR is fixed at 26.50 dB. Note that this SNR corresponds to the case where the information rate reaches around 4.250 in bits per dimension, which corresponds to the rate achieved by 32-PAM with an ideal rate-17/20 channel code. It is observed that the maximum value of nearly 4.262 is reached at $\alpha = 0.882$ in the case of CM capacity. Similarly, the maximum value of 4.256 is achieved with $\alpha = 0.874$ for BICM capacity. Thus, in what follows, we refer to the constellations obtained with these parameters as the optimal constellations for each respective coded modulation scheme.

The constellation constrained capacities among several representative 32-PAM constellations are compared in Fig. 6 within the SNR range where the information rate is around 4.250 in bits per dimension. It can be observed that the CDF-based Gaussian-like constellation is superior to the centroid-based constellation, and these Gaussian-like constellations are attractive in relatively low SNR regions when compared to the standard (uniformly-spaced) constellation. However, the proposed constellation based on the truncated Gaussian with the selected parameter outperforms the others for the information rate range of interest. In Section V, we will investigate the error rate performance of the proposed constellations by extensive simulations employing practical coded modulation schemes. Since we employ M^2-QAM symbols consisting of the two identical M-PAM symbols in practice, the total achievable information rate of the entire system should be doubled.

Coded modulation based on non-uniform high-order PAM has also been investigated in [35], where a geometric shaping approach based on binomial distribution is introduced. In their approach, $m = \log_2 M$ parameters need to be optimized to determine M-ary PAM constellation. In Fig. 7,

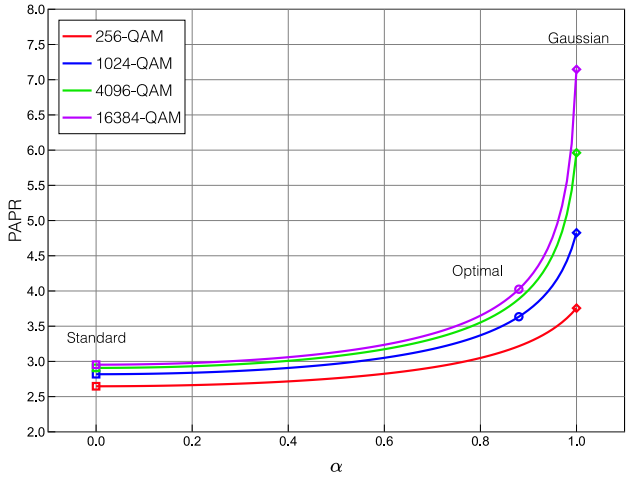

FIGURE 8. PAPR versus the parameter α in the proposed constellation design; Square points and diamond points correspond to the cases of the standard QAM and CDF-based Gaussian-like QAM, respectively. Also, the circles represent those with the constellations optimized at their target SNR values (i.e., $\alpha = 0.882$ for 1024-QAM and $\alpha = 0.884$ for 16384-QAM, as discussed in Section V).

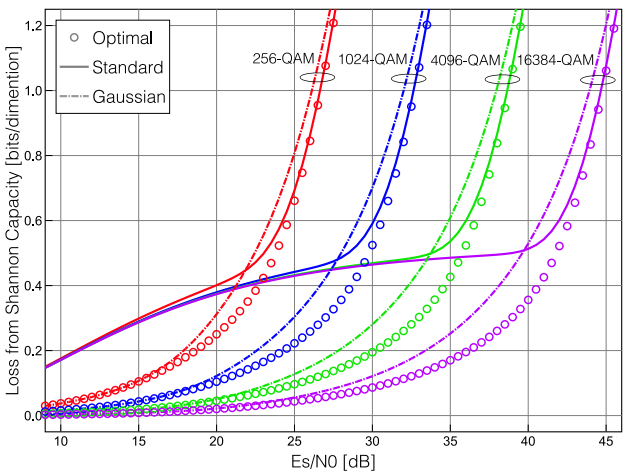

FIGURE 9. Comparison of the loss of the achievable information rate from the Shannon limit with modulation sizes $M^2 = 256, 1024, 4096, 16384$.

the constellation constrained capacity of our proposed 256-PAM is compared with that of [35], where each constellation is optimized at SNR of 30.10 [dB]. The result indicates that our proposed PAM as well as Gaussian PAM outperform that based on [35], even though the proposed systematic design approach requires much less parameters to be optimized.

2) PAPR ANALYSIS

In general, geometrically shaped constellations often have higher PAPR, which is a well-known major drawback since it results in poor power amplifier efficiency [42]. Thus, we should take this issue into account when designing constellation in practice. For a given set of discrete constellation points with normalized energy, the PAPR of the proposed constellation is expressed as [43]

$$\begin{aligned}\mathrm{PAPR} &= \max_{k,l}|a_k + ja_l|^2 = 2a_0^2 \\ &= \frac{M\,\mathrm{erf}^{-1}\left(\alpha\left(\frac{1}{M}-1\right)\right)}{\sum_{k=0}^{M-1}\mathrm{erf}^{-1}\left(\alpha\left(\frac{2k+1}{M}-1\right)\right)},\end{aligned} \tag{31}$$

which will be determined only by the two parameters α and M. For several representative values of M, the transition of the PAPR with respect to the design parameter α is shown in Fig. 8, where it is apparent that the PAPR of the Gaussian-like constellations rapidly grows with M, while that of the standard constellations (i.e., $\alpha = 0$) saturates at its upper limit of 3 [43]. This is one of the major practical issues associated with the constellation design based on Gaussian distribution. As for the proposed design, the resulting PAPR depends on the value of α, and the constellations optimized at their target SNR values have much lower values than the Gaussian-like constellations (i.e., $\alpha = 1$), despite the fact that they potentially improve the achievable error rate performance.

3) LOSS FROM OPTIMAL CONSTELLATION

We discuss the applicability of our proposed shaping approach to systems operating with various modulation sizes and information rates in terms of the loss of the achievable information rate by a given constellation set $\mathcal{A}$ from the corresponding Shannon limit evaluated at specific SNR [20]. It is defined as

$$L\left(\mathcal{A}, \frac{E_s}{N_0}\right) \triangleq \log_2\left(1+\frac{E_s}{N_0}\right) - 2C_{\mathrm{CM}}\left(\mathcal{A}, \frac{E_s}{N_0}\right) \tag{32}$$

in bits per symbol, where the second term corresponds to the two-dimensional coded modulation capacity. The results in the cases of $M^2 = 256, 1024, 4096$, and 16384 are shown in Fig. 9, where it can be confirmed that the proposed shaping approach is effective for all the modulation sizes. Furthermore, compared to the standard QAM, reduction in the loss from the Shannon limit achieved by the optimized case becomes significant as the constellation size increases. Therefore, the use of shaping approach would be beneficial especially for the transmission systems with high information rate, which is the main focus of this work.

There have been a growing number of studies on geometrical shaping optimization over two or higher-dimensional constellation cases such as [30], [31], and [32]. In [30], a rigorous constellation optimization algorithm for two and higher dimensional cases is proposed and it is shown to achieve remarkable shaping gains over a wide range of SNRs. In order to make a comparison with [30] in a practical coded modulation scenario, we also evaluate the loss of the achievable information rate in the case of BICM calculated using (32) with C_{CM} replaced by C_{BICM}. (Note that the BICM capacity of the proposed constellation is discussed later in Section IV-B.) The results are shown in Fig. 10, where that of a two-dimensional constellation in the case of 1024 points, optimized at an SNR of 26.00 dB according to [44], is also plotted. We observe that our proposed 1024-QAM designed by optimizing one-dimensional constellation

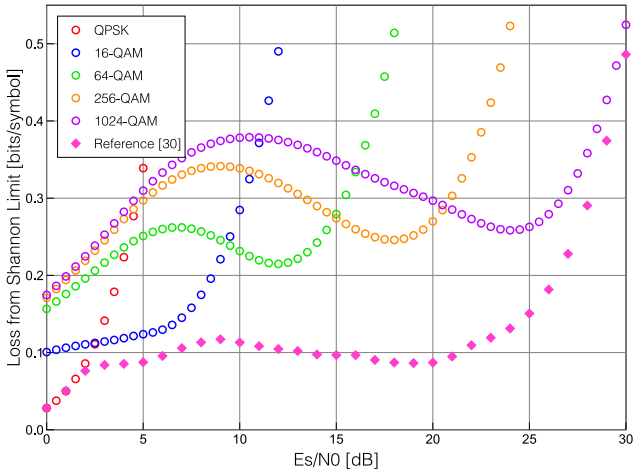

FIGURE 10. Loss of the achievable information rate from the Shannon limit in the case of BICM with the proposed constellations. The case of the two-dimensional constellation with 1024 points proposed in [30] is also plotted.

has a gap of 0.279 bits per symbol from the limit at the SNR of 26.00 dB, whereas that of [44] is as low as 0.182 bits per symbol, indicating the limitation of our one-dimensional approach. Nevertheless, the shaping gain achieved by the proposed constellations should remain beneficial when one considers practical issues such as computational cost required for demapping operation as well as their applicability to MLC/MSD without major modifications, which will be discussed in the subsequent sections.

IV. CODED MODULATION SCHEMES AND THEIR DESIGN

In the previous section, we have shown that the proposed constellation shaping can achieve the gain over the standard QAM constellation from a viewpoint of the resulting constellation constrained capacity and the bit-wise mutual information. In order to investigate their achievable performance in terms of bit error rate with actual channel coding, practical coded modulation schemes should be applied. In this section, we investigate the application of two representative coded modulation schemes to the proposed shaping system.

A. MULTILEVEL CODING AND MULTISTAGE DECODING

Multilevel coding (MLC) with multistage decoding (MSD) [15] has been shown to approach the constellation constrained capacity using multiple binary channel codes [17]. In what follows, we briefly review MLC/MSD design based on the capacity rule [17], which will be employed with our proposed geometric shaping.

1) MULTILEVEL CODING (MLC) AND MULTISTAGE DECODING (MSD)

We consider the MLC transmitter employing a given constellation $\mathcal{A}$ with cardinality $|\mathcal{A}| = M = 2^m$. A binary information sequence $\boldsymbol{q}$ is first partitioned into m binary subsequences denoted by $\boldsymbol{q}^{(i)}$, $i \in \{0, 1, \ldots, m-1\}$. Each binary subsequence $\boldsymbol{q}^{(i)}$ of length K_i is encoded by a different binary component code to generate a codeword $\boldsymbol{c}^{(i)} = (c_0^{(i)}, c_1^{(i)}, \ldots, c_{N-1}^{(i)})$ of length N with its code rate given by $R_i = K_i/N$. Each element of m codewords is combined to form $\boldsymbol{c}_n = (c_n^{(0)}, c_n^{(1)}, \ldots, c_n^{(m-1)})$ for $n \in \{0, 1, \ldots, N-1\}$ and then mapped onto the corresponding constellation point chosen from $\mathcal{A}$, which will be transmitted over an AWGN channel. The information rate R of the entire system (bits per dimension) is given by

$$R = R_0 + R_1 + \cdots + R_{m-1}. \tag{33}$$

At the receiver side, decoding is performed sequentially from the lowest level until all the codewords in m levels are decoded.

2) EQUIVALENT CHANNEL

Let $X \in \mathcal{A}$ denote a random variable representing a transmitted symbol and let $X^0, X^1, \ldots, X^{m-1} \in \mathbb{F}_2^m$ denote its binary representation (corresponding to $\boldsymbol{c}_n$). The mutual information of X and its received symbol Y over an AWGN channel can be expressed as

$$\begin{aligned} C_{\mathrm{CM}} &= I(Y; X) \\ &= I\Big(Y; X^0, X^1, \ldots, X^{m-1}\Big). \end{aligned} \tag{34}$$

The application of the chain rule [45] to the above equation yields

$$\begin{aligned} C_{\mathrm{CM}} = \underbrace{I\Big(Y; X^0\Big)}_{\triangleq C_0} + \underbrace{I\Big(Y; X^1 | X^0\Big)}_{\triangleq C_1} \\ + \cdots + \underbrace{I\Big(Y; X^{m-1} | X^0, X^1, \ldots, X^{m-2}\Big)}_{\triangleq C_{m-1}}. \end{aligned} \tag{35}$$

The above equation implies that, provided that all the bits in the lower levels are known, the transmission of MLC can be regarded as the parallel transmission of the binary symbols $(X^0, X^1, \ldots, X^{m-1})$ over the m independent *equivalent channels*. As a result, the capacity of the ith equivalent channel is given by

$$C_i = I\Big(Y; X^i | X^0, X^1, \ldots, X^{i-1}\Big) \tag{36}$$

for $i \in \{1, 2, \ldots, m-1\}$.

3) RATE DESIGN BASED ON CAPACITY RULE

According to the capacity rule [17], the rates of the component codes should satisfy

$$R_i \leq C_i. \tag{37}$$

The information rate R of (33) can be achieved as long as (37) holds for all levels. In principle, by setting R_i equal to C_i, one can achieve the constellation constrained capacity C_{CM} by MLC/MSD. In practice, however, some rate loss would be unavoidable due to the lack of flexibility in component code design as well as a limitation of the codeword length.

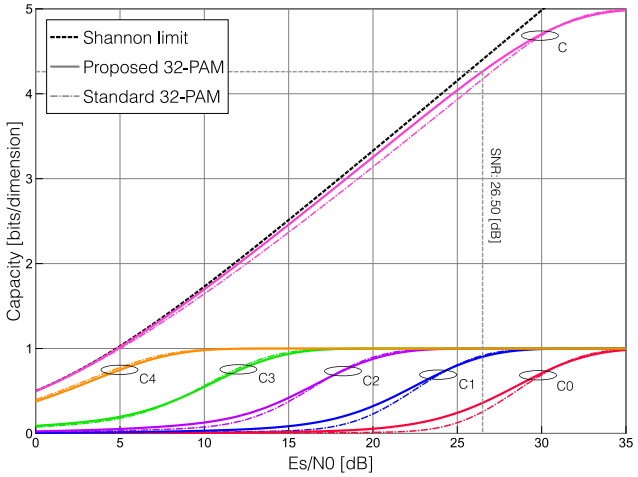

FIGURE 11. The equivalent channel capacities for the proposed 32-PAM (solid lines) and the standard 32-PAM (dot-dashed lines).

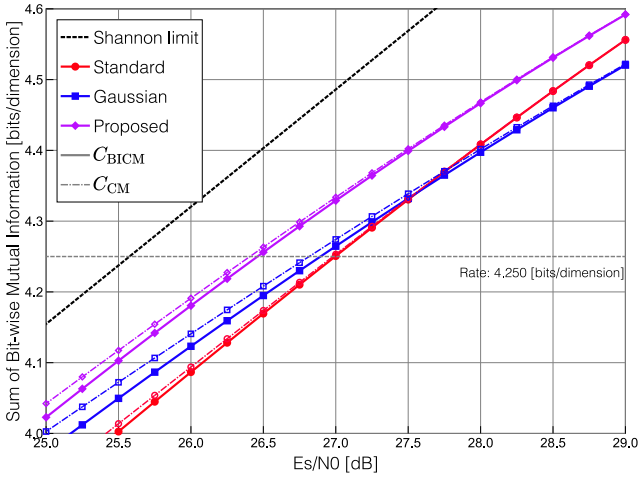

FIGURE 12. Comparison of C_{BICM} and C_{CM} for various 32-PAM constellations.

4) DESIGN EXAMPLE

The equivalent channel capacities over an AWGN channel for the proposed 32-PAM constellation ($\alpha = 0.882$) with natural labeling are numerically calculated and plotted in Fig. 11 as solid lines, whereas those of the standard 32-PAM are also plotted as dot-dashed lines for reference. The vertical line indicates the SNR of 26.50 dB, at which we will design and compare our system through simulations in Section V. It is observed that MLC/MSD achieves the information rate of around $C_{\mathrm{CM}} = 4.262$ at this SNR, where the resulting rates of the component codes are given by $C_0 = 0.360, C_1 = 0.902, C_2 = 0.999$, and $C_3 = C_4 = 1.000$. From this result, we observe that the two highest equivalent channels can be left uncoded, which is beneficial in terms of practical receiver implementation.

B. BIT-INTERLEAVED CODED MODULATION

Bit-interleaved coded modulation (BICM) [14] is a simple coded modulation scheme which uses only a single chain of channel encoder and decoder. BICM can be modeled as a serial concatenation of encoder, random bit-wise interleaver, and signal mapper.

At the transmitter, the entire information sequence $\boldsymbol{q}$ is encoded by a single encoder. The codeword $\boldsymbol{c}$ is bit-wise interleaved and then mapped onto the corresponding signal point from a constellation set $\mathcal{A}$.

1) BICM CAPACITY

Similar to MLC/MSD, BICM decomposes each symbol consisting of 2^m constellation points into m binary channels, where these binary channels are combined through random bit interleaver. As a result, BICM enjoys simplified design and implementation, but the price is its loss in terms of achievable information rate compared to C_{CM} since all the binary channels are treated as independent.

The corresponding mutual information is expressed as [16]

$$C_{\mathrm{BICM}} = m - \sum_{i=0}^{m-1} \mathbb{E}_{Y,B_i}\left[\log_2 \frac{\sum_{x\in\mathcal{A}} p_{Y|X}(Y \mid x)}{\sum_{x\in\mathcal{A}_{B_i}^{(i)}} p_{Y|X}(Y \mid x)}\right], \quad (38)$$

where $B_i \in \mathbb{F}_2$ is a random variable representing the bit of the ith binary channel, and $\mathcal{A}_b^{(i)}$ denotes the set of constellations in the ith binary channel with the bit specified by $b \in \mathbb{F}_2$. The gap between C_{CM} and C_{BICM} is significantly affected by bit labeling schemes that determine $\mathcal{A}_b^{(i)}$ for $i \in \{0, 1, \ldots, m-1\}$, and in high SNR regime it is well known that the binary reflected Gray code (BRGC) becomes optimal for the standard QAM constellations [46]. As for the Gaussian-like constellations, the optimization of bit-labeling has been studied in [22], and through numerical analysis it turned out that BRGC still achieves the best performance across a wide range of SNRs. Thus, we adopt BRGC for all the constellations employed in BICM throughout this work.

2) NUMERICAL EXAMPLE

Fig. 12 compares C_{BICM} (solid lines) and C_{CM} (dot-dashed lines) for various 32-PAM constellations considered in this work. By comparing all the curves corresponding to C_{BICM}, we observe that significant shaping gain (from the standard constellation) can be expected even for BICM. It can also be observed that when we focus on the information rate of 4.250 in bits per dimension, each gap between C_{BICM} and C_{CM} is relatively small, indicating that they may perform similarly when they are designed targeting relatively high information rate.

V. SIMULATION RESULTS

In this section, we evaluate the performance of our proposed constellation shaping in combination with MLC/MSD and BICM in terms of their bit error rate (BER) performance through computer simulation. The simulation parameters adopted are listed in Table 1. The corresponding PAPR values are indicated by the circles in Fig. 8.

TABLE 1. Simulation parameters.

Coded Modulation	MLC/MSD or BICM
Bit labeling	MLC: Natural labeling BICM: Gray labeling
Selected parameter (proposed constellation)	32-PAM (1024-QAM) MLC: $\alpha = 0.882$ BICM: $\alpha = 0.874$ 128-PAM (16 384-QAM) MLC: $\alpha = 0.884$ BICM: $\alpha = 0.878$
Channel coding	Turbo code
Decoding	Log-MAP (iteration: 15)
Code rate	$R = 17/20$ for 32-PAM $R = 22/25$ for 128-PAM
Codeword length	MLC: 7000 (each level) BICM: 7000
Channel	AWGN

TABLE 2. Code rates of component codes in MLC systems.

32-PAM (1024-QAM)

Level	R_0	R_1	R_2	R_3, R_4	R
Rate	9/25	9/10	99/100	1 (uncoded)	17/20

128-PAM (16 384-QAM)

Level	R_0	R_1	R_2	R_3, R_4, R_5, R_6	R
Rate	33/100	21/25	99/100	1 (uncoded)	22/25

A. CODE RATE DESIGN

In all the simulations, we employ the original rate-1/3 turbo coding, where the code rates are adjusted by rate-compatible puncturing [47]. In our simulations for 32-PAM (1024-QAM), we set the code rate as $R = 17/20$ leading to the spectral efficiency of 4.250 in bits per dimension. This corresponds to the case discussed in Section III-C. For 128-PAM (16 384-QAM) with $R = 22/25$, the resulting spectral efficiency is 6.16 in bits per dimension.

For MLC, we should adjust the code rate of each level according to the equivalent channel capacity, shown in Fig. 11 in the case of 32-PAM (1024-QAM). Consequently, we set $R_0 = 9/25, R_1 = 9/10$, and $R_2 = 99/100$, whereas $R_3 = R_4 = 1$ (uncoded) for 32-PAM. As for 128-PAM (16 384-QAM), the number of levels is $m = 7$ per dimension and the rates are determined by the same process as that of 32-PAM (1024-QAM). The resulting rates that we found are summarized in Table 2 for both cases.

B. BER RESULTS

The BER performances of the standard 32-PAM (1024-QAM) and the proposed shaping with optimal parameters are compared in Fig. 13, where MLC/MSD and BICM are applied to both the systems. As expected, we observe that MLC/MSD outperforms BICM when compared at a BER around 10^{-4}. Furthermore, for both systems, the proposed

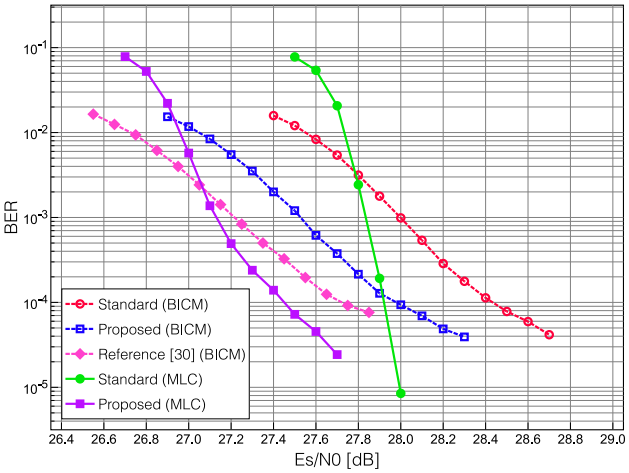

FIGURE 13. Comparison of BER performances between the standard and proposed 32-PAM (1024-QAM) constellations with MLC/MSD and BICM. The case for BICM employing the two-dimensional constellation proposed in [30] with the same cardinality is also depicted.

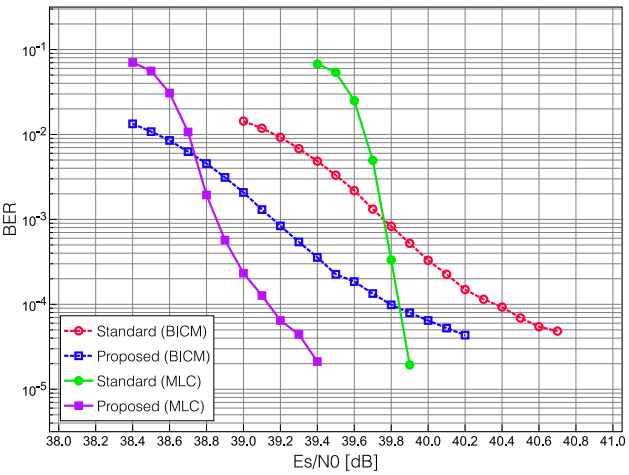

FIGURE 14. Comparison of BER performances between the standard and proposed 128-PAM (16384-QAM) constellations with MLC/MSD and BICM.

constellation shaping significantly improves the performance over the standard constellations. The BER performance of the BICM employing the two-dimensional designed constellation with 1024 points is also shown in the figure, where we observe that this constellation achieves the best performance among BICM systems. However, our proposed MLC through one-dimensional optimization still reaches a BER of 10^{-4} at the lowest SNR among all systems compared here.

Furthermore, the case of 128-PAM (16384-QAM) constellations are compared in Fig. 14, where we observe the same tendency as that of 32-PAM (1024-QAM) in Fig. 13, indicating that the proposed shaping can be systematically designed even for QAM constellations of an arbitrary large size. It is also interesting to observe that the shaping gains become more visible with the larger number of constellation points.

VI. COMPLEXITY COMPARISON

Finally, we compare MLC/MSD and BICM from the viewpoint of decoding complexity. We here focus on computational complexity associated with bit metric calculation as it is independent of coding schemes employed. Note that there have been various researches on simplified soft-output demappers for both single-dimensional and two-dimensional constellations [48], [49], [50]. However, since these approaches typically rely on unique structure of specific geometrical constellations, we focus on the conventional bit LLR calculation in view of generality.

A. GENERAL TWO-DIMENSIONAL CONSTELLATION

Let us assume that transmitted symbols are chosen from a given set of complex-valued (i.e., two-dimensional) constellation points $\mathcal{A}$, where its cardinality is given by $|\mathcal{A}| = 2^{2m}$ with a positive integer m. Then the complexity should be measured by the numbers of multiplications, additions, and comparisons required for calculating $2m$ LLR values in one transmitted symbol.

Since the exact calculation of LLR values becomes computationally demanding as the constellation size increases, the LLR value of the ith bit level is commonly approximated by

$$L_i = \log\left[\frac{\sum_{a\in\mathcal{A}_0^{(i)}} \exp\left(-\frac{|y-a|^2}{2\sigma^2}\right)}{\sum_{a\in\mathcal{A}_1^{(i)}} \exp\left(-\frac{|y-a|^2}{2\sigma^2}\right)}\right] \tag{39}$$

$$\approx \min_{a\in\mathcal{A}_0^{(i)}}\left\{|y-a|^2\right\} - \min_{a\in\mathcal{A}_1^{(i)}}\left\{|y-a|^2\right\}, \tag{40}$$

where $y \in \mathbb{C}$ represents the received complex-valued symbol. From the above equation, it is necessary to calculate the squared Euclidean distances between the received symbol and all of $|\mathcal{A}|$ constellation points. This process requires $2|\mathcal{A}|$ real multiplications and $|\mathcal{A}|$ real additions. Then, one has to compare these values in order to identify the minimum values associated with the subsets $\mathcal{A}_0^{(i)}$ and $\mathcal{A}_1^{(i)}$. The corresponding number of comparison operations, denoted by N_c, can be expressed as

$$N_c = \left(\log_2|\mathcal{A}|\right)\sum_{i=0}^{\log_2|\mathcal{A}|}\left(\left|\mathcal{A}^{(i)}\right| - 2\right), \tag{41}$$

where $\mathcal{A}^{(i)} \triangleq \mathcal{A}_0^{(i)} \cup \mathcal{A}_1^{(i)}$ is the (sub)set of the constellation points associated with the ith bit level, and we thus have $|\mathcal{A}^{(i)}| = |\mathcal{A}_0^{(i)}| + |\mathcal{A}_1^{(i)}|$ since the subsets $\mathcal{A}_0^{(i)}$ and $\mathcal{A}_1^{(i)}$ are mutually exclusive in general. Finally, $\log_2|\mathcal{A}|$ additions are required to complete the entire LLR calculation process.

Since $\mathcal{A}^{(i)} = \mathcal{A}$ for all the bit levels in the case of BICM, we have $|\mathcal{A}^{(i)}| = |\mathcal{A}|$. On the other hand, for MLC/MSD, the number of constellation points decreases as the bit level i increases. Specifically, the cardinality of $\mathcal{A}^{(i)}$ becomes half of that of its lower level $\mathcal{A}^{(i-1)}$, and thus we have $|\mathcal{A}^{(i)}| = |\mathcal{A}|/2^i$ for the ith bit level. Therefore, the required number of comparisons for MLC/MSD is significantly lower than that of BICM in higher spectral efficiency regime.

TABLE 3. The numbers of several operations required for calculating $2m$ LLR values per one transmitted symbol. Numerical values correspond to the case with $m = 7$ (i.e., 16384-QAM).

General two-dimensional constellations where $|\mathcal{A}| = 2^{2m}$

	MLC/MSD	BICM
Mul.	2^{2m+1} $(= 32768)$	2^{2m+1} $(= 32768)$
Add.	$2^{2m} + 2m$ $(= 16398)$	$2^{2m} + 2m$ $(= 16398)$
Com.	$2\left(2^{2m} - 2m - 1\right)$ $(= 32738)$	$2m\left(2^{2m} - 2\right)$ $(= 229348)$

Two independent PAM constellations

	MLC/MSD	BICM
Mul.	$2 \cdot 2^{m+1}$ $(= 512)$	$2 \cdot 2^{m+1}$ $(= 512)$
Add.	$2 \cdot (2^m + m)$ $(= 270)$	$2 \cdot (2^m + m)$ $(= 270)$
Com.	$2 \cdot 2\,(2^m - m - 1)$ $(= 480)$	$2 \cdot m\,(2^m - 2)$ $(= 1764)$

B. TWO INDEPENDENT PAM CONSTELLATIONS

In this work, we have exclusively focused on the system where each of in-phase and quadrature channels consists of an independent one-dimensional constellation. Therefore, the number of the constellation points per each dimension is the square root of that of the two-dimensional constellation, i.e., $|\mathcal{A}| = 2^m$, which leads to significant reduction of the overall computational complexity compared to the general two-dimensional case described above.

C. DISCUSSION

The numbers of mathematical operations required in MLC/MSD and BICM decoders are summarized in Table 3 as functions of m, where we consider the following four cases: MLC/MSD and BICM with general two-dimensional constellations and those based on two independent one-dimensional constellations. Note that the specific numbers shown on the right side indicate the cases with $m = 7$, thus leading to $|\mathcal{A}| = 2^{14} = 16\,384$. When we focus on one-dimensional systems, it can be confirmed that the number of comparisons required in MLC/MSD is about 27% of that of BICM, and thus MLC/MSD has much less decoding complexity in addition to its superior error rate performance.

Constellations designed in two or even higher dimensions, such as those proposed in [30], [31], and [32], have their significant shaping gains, but the price is their required computational complexity for decoding, especially when BICM is employed. From all the above results, we may conclude that MLC/MSD with our proposed one-dimensional shaping approach should achieve well-balanced trade-off between the error rate performance (including shaping gain) and decoding complexity, which should be attractive from a viewpoint of practical coded modulation implementation.

VII. CONCLUSION

In this paper, we have proposed a systematic geometrical constellation shaping for high-order QAM designed according to the truncated Gaussian distribution and evaluated its achievable BER performance in the framework of MLC/MSD and BICM.

The simulation results of the proposed system employing practical off-the-shelf binary punctured turbo codes indicate that the effective shaping gains can readily be achieved even with a low-complexity parameter optimization. Furthermore, MLC/MSD can offer better BER performance as well as decoding simplicity compared to BICM, provided that the code rates of their equivalent binary channels are properly designed.

As future work, the application of the proposed shaping to adaptive modulation would be of significant practical interest. Furthermore, the impact of high PAPR caused by shaping operation in the presence of power amplifier nonlinearity should be investigated.

REFERENCES

[1] P. K. Singya, P. Shaik, N. Kumar, V. Bhatia, and M.-S. Alouini, "A survey on higher-order QAM constellations: Technical challenges, recent advances, and future trends," *IEEE Open J. Commun. Soc.*, vol. 2, pp. 617–655, 2021.

[2] G. Forney, R. Gallager, G. Lang, F. Longstaff, and S. Qureshi, "Efficient modulation for band-limited channels," *IEEE J. Se. Areas. Commun.*, vol. 2, no. 5, pp. 632–647, Sep. 1984.

[3] J. Cho and P. J. Winzer, "Probabilistic constellation shaping for optical fiber communications," *J. Lightw. Technol.*, vol. 37, no. 6, pp. 1590–1607, Mar. 15, 2019.

[4] S. Y. Le Goff, B. K. Khoo, C. C. Tsimenidis, and B. S. Sharif, "Constellation shaping for bandwidth-efficient turbo-coded modulation with iterative receiver," *IEEE Trans. Wireless Commun.*, vol. 6, no. 6, pp. 2223–2233, Jun. 2007.

[5] M. C. Valenti and X. Xiang, "Constellation shaping for bit-interleaved LDPC coded APSK," *IEEE Trans. Commun.*, vol. 60, no. 10, pp. 2960–2970, Oct. 2012.

[6] R. T. Jones, T. A. Eriksson, M. P. Yankov, and D. Zibar, "Deep learning of geometric constellation shaping including fiber nonlinearities," in *Proc. Eur. Conf. Opt. Commun. (ECOC)*, 2018, pp. 1–3.

[7] A. I. Abd El-Rahman and J. C. Cartledge, "Multidimensional geometric shaping for QAM constellations," in *Proc. Eur. Conf. Opt. Commun. (ECOC)*, 2017, pp. 1–3.

[8] G. Böcherer, F. Steiner, and P. Schulte, "Bandwidth efficient and rate-matched low-density parity-check coded modulation," *IEEE Trans. Commun.*, vol. 63, no. 12, pp. 4651–4665, Dec. 2015.

[9] T. Matsumine, T. Koike-Akino, and H. Ochiai, "A low-complexity probabilistic amplitude shaping with short linear block codes," *IEEE Trans. Commun.*, vol. 69, no. 12, pp. 7923–7933, Dec. 2021.

[10] Y. C. Gültekin, W. J. van Houtum, A. G. C. Koppelaar, F. M. J. Willems, and W. J. van Houtum, "Enumerative sphere shaping for wireless communications with short packets," *IEEE Trans. Wireless Commun.*, vol. 19, no. 2, pp. 1098–1112, Feb. 2020.

[11] F. A. Aoudia and J. Hoydis, "Joint learning of probabilistic and geometric shaping for coded modulation systems," in *Proc. IEEE Glob. Commun. Conf. (GLOBECOM)*, 2020, pp. 1–6.

[12] M. Stark, F. A. Aoudia, and J. Hoydis, "Joint learning of geometric and probabilistic constellation shaping," in *Proc. IEEE Glob. Commun. Conf. (GLOBECOM)*, 2019, pp. 1–6.

[13] E. Zehavi, "8-PSK trellis codes for a Rayleigh channel," *IEEE Trans. Commun.*, vol. 40, no. 5, pp. 873–884, May 1992.

[14] G. Caire, G. Taricco, and E. Biglieri, "Bit-interleaved coded modulation," *IEEE Trans. Inf. Theory*, vol. 44, no. 3, pp. 927–946, May 1998.

[15] H. Imai and S. Hirakawa, "A new multilevel coding method using error-correcting codes," *IEEE Trans. Inf. Theory*, vol. 23, no. 3, pp. 371–377, May 1977.

[16] L. Szczecinski and A. Alvarado, *Bit-Interleaved Coded Modulation: Fundamentals, Analysis and Design*. Hoboken, NJ, USA: Wiley, 2015.

[17] U. Wachsmann, R. F. Fischer, and J. B. Huber, "Multilevel codes: Theoretical concepts and practical design rules," *IEEE Trans. Inf. Theory*, vol. 45, no. 5, pp. 1361–1391, Jul. 1999.

[18] G. Ungerboeck, "Channel coding with multilevel/phase signals," *IEEE Trans. Inf. Theory*, vol. 28, no. 1, pp. 55–67, Jan. 1982.

[19] T. Matsumine, M. P. Yankov, and S. Forchhammer, "Geometric constellation shaping for concatenated two-level multi-level codes," *IEEE J. Lightw. Technol.*, vol. 40, no. 16, pp. 5557–5566, Aug. 15, 2022.

[20] G. Montorsi, "Design of constellation sets for multistage systems," in *Proc. IEEE Glob. Commun. Conf. (GLOBECOM)*, 2016, pp. 1–6.

[21] T. Koike-Akino, Y. Wang, S. C. Draper, K. Sugihara, and W. Matsumoto, "Bit-interleaved polar-coded OFDM for low-latency M2M wireless communications," in *Proc. IEEE Int. Conf. Commun (ICC)*, 2017, pp. 1–7.

[22] B. Wiens and D. C. Lee, "Performance variation of gray codes for cropped Gaussian 16PAM constellations," in *Proc. IEEE Mil. Commun. Conf. (MILCOM)*, 2022, pp. 89–94.

[23] F. Kayhan and G. Montorsi, "Joint signal-labeling optimization under peak power constraint," *Int. J. Satell. Commun. Netw.*, vol. 30, no. 6, pp. 251–263, 2012.

[24] F. Kayhan and G. Montorsi, "Constellation design for memoryless phase noise channels," *IEEE Trans. Wireless Commun.*, vol. 13, no. 5, pp. 2874–2883, May 2014.

[25] J. Barrueco et al., "Constellation design for bit-interleaved coded modulation (BICM) systems in advanced broadcast standards," *IEEE Trans. Broadcast.*, vol. 63, no. 4, pp. 603–614, Dec. 2017.

[26] F. Jerji, C. Akamine, and N. Omar, "Designing non-uniform constellations using genetic algorithm," in *Proc. IEEE Int. Symp. Broadband Multimed. Syst. Broadcast. (BMSB)*, 2020, pp. 1–5.

[27] R. T. Jones et al., "Geometric constellation shaping for fiber optic communication systems via end-to-end learning," 2018, *arXiv:1810.00774*.

[28] V. Aref and M. Chagnon, "End-to-end learning of joint geometric and probabilistic constellation shaping," in *Proc. Optic. Fiber Commun. Conf. Exhib. (OFC)*, 2022, pp. 1–3.

[29] B. Wiens and D. C. Lee, "Constellation design with equal-probability partition of a cropped Gaussian distribution," in *Proc. IEEE 92nd Veh. Technol. Conf. (VTC-Fall)*, 2020, pp. 1–5.

[30] E. Sillekens, G. Liga, D. Lavery, P. Bayvel, and R. I. Killey, "High-cardinality geometrical constellation shaping for the nonlinear fibre channel," *J. Lightw. Technol.*, vol. 40, no. 19, pp. 6374–6387, Oct. 1, 2022.

[31] K. Gümüş, B. Chen, T. Bradley, and C. Okonkwo, "A simplified method for optimising geometrically shaped constellations of higher dimensionality," 2023, *arXiv:2307.05179*.

[32] B. Chen et al., "Geometrically-shaped multi-dimensional modulation formats in coherent optical transmission systems," *J. Lightw. Technol.*, vol. 41, no. 3, pp. 897–910, Feb. 1, 2023.

[33] M. Tanahashi and H. Ochiai, "A multilevel coded modulation approach for hexagonal signal constellation," *IEEE Trans. Wireless Commun.*, vol. 8, no. 10, pp. 4993–4997, Oct. 2009.

[34] D. Yoda and H. Ochiai, "Multilevel coded modulation with reduced latency decoding based on novel set partitioning for APSK," *IEEE Trans. Broadcast.*, vol. 61, no. 4, pp. 674–684, Dec. 2015.

[35] H. S. Cronie, "Superposition coding for power-and bandwidth efficient communication over the Gaussian channel," in *Proc. IEEE Int. Symp. Inf. Theory (ISIT)*, 2007, pp. 2311–2315.

[36] C. Ji, J. Wang, and G. Zhang, "Approximate expression for the mutual information of dense PAM," *IEEE Commun. Lett.*, vol. 22, no. 11, pp. 2182–2185, Nov. 2018.

[37] M. Urlea and S. Loyka, "Simple closed-form approximations for achievable information rates of coded modulation systems," *J. Lightw. Technol.*, vol. 39, no. 5, pp. 1306–1311, Mar. 1, 2021.

[38] J. A. López-Salcedo and G. Vázquez, "Closed-form upper bounds for the constellation-constrained capacity of ultra-wideband communications," in *Proc. IEEE Int. Conf. Acoust, Speech Signal Process. (ICASSP)*, vol. 3, 2007, pp. 565–568.

[39] E. Kurihara and H. Ochiai, "A systematic constellation design for BICM systems with geometric shaping," in *Proc. IEEE Consum. Commun. Netw. Conf. (CCNC)*, 2023, pp. 1048–1053.

[40] F.-W. Sun and H. C. A. van Tilborg, "Approaching capacity by equiprobable signaling on the Gaussian channel," *IEEE Trans. Inf. Theory*, vol. 39, no. 5, pp. 1714–1716, Sep. 1993.

[41] J. J. Boutros, U. Erez, J. Van Wonterghem, G. I. Shamir, and G. Zémor, "Geometric shaping: Low-density coding of Gaussian-like constellations," in *Proc. IEEE Inf. Theory Wksp. (ITW)*, 2018, pp. 1–5.

[42] H. Ochiai, "An analysis of band-limited communication systems from amplifier efficiency and distortion perspective," *IEEE Trans. Commun.*, vol. 61, no. 4, pp. 1460–1472, Apr. 2013.

[43] H. Ochiai, "Exact and approximate distributions of instantaneous power for pulse-shaped single-carrier signals," *IEEE Trans. Wireless Commun.*, vol. 10, no. 2, pp. 682–692, Feb. 2011.

[44] E. Sillekens, G. Liga, D. Lavery, P. Bayvel, and R. I. Killey, "High-cardinality geometrically shaped constellation for the aWGN channel and optical fibre channel," Dataset, University College London. Accessed: May 20, 2024. [Online]. Available: https://doi.org/10.5522/04/20223963.v1

[45] R. G. Gallager, *Information Theory and Reliable Communication*. New York, NY, USA: Wiley, 1968.

[46] A. Alvarado, F. Brännström, E. Agrell, and T. Koch, "High-SNR asymptotics of mutual information for discrete constellations with applications to BICM," *IEEE Trans. Inf. Theory*, vol. 60, no. 2, pp. 1061–1076, Feb. 2014.

[47] J. Li, Q. Chen, S. Gao, Z. Ma, and P. Fan, "The optimal puncturing pattern design for rate-compatible punctured turbo codes," in *Proc. Int. Conf. Wireless Commun. Signal Process. (WCSP)*, 2009, pp. 1–5.

[48] I.-W. Kang, J.-W. Shin, and H.-N. Kim, "Low-complexity LLR calculation for gray-coded PAM modulation," *IEEE Commun. Lett.*, vol. 20, no. 4, pp. 688–691, Apr. 2016.

[49] H. Hong, Y. Xu, Y. Wu, D. He, N. Gao, and W. Zhang, "Backward compatible low-complexity demapping algorithms for two-dimensional non-uniform constellations in ATSC 3.0," *IEEE Trans. Broadcast.*, vol. 67, no. 1, pp. 46–55, Mar. 2021.

[50] J. Barrueco, J. Montalban, P. Angueira, C. A. Nour, and C. Douillard, "Low complexity adaptive demapper for 2-D non-uniform constellations," *IEEE Trans. Broadcast.*, vol. 65, no. 1, pp. 10–19, Mar. 2019.